Effect of Sodium Alginate on Properties of Wheat Straw/Polylactic Acid Composites

Xuanhao Zhang *

To investigate the effect of sodium alginate (SA) on the properties of wheat straw/polylactic acid (PLA) composites, four kinds of composites with different SA contents (0 wt%, 5 wt%, 10 wt%, and 15 wt%) were prepared *via* injection molding. The mechanical properties, moisture absorption, thermal stability, and infrared spectrum of the four kinds of composites were tested and analyzed, and the microstructure of the tensile section of the composites was observed via scanning electron microscopy. The degradability of the composites was also analyzed. The results showed that the wheat straw/PLA composites with 5% SA had better mechanical properties. Their tensile strength was 15.8%, 5.4%, and 19% higher than those of 0%, 10%, and 15% SA, respectively. The impact strength of the 5% SA composites changed to an acceptable degree relative to the non-SA composites, which had an impact strength of 28% lower than that of 0% SA but 51.9% higher than that of the 15% SA composite. The 5% SA composites had less hygroscopicity and better thermal stability, and adding SA enhanced the degradability of the composites. As the SA content increased, degradability increased greatly.

Keywords: Polylactic acid; Sodium alginate; Biocomposites; Mechanical properties; Hygroscopicity; Degradability; Thermal stability

Contact information: College of Engineering, Nanjing Agricultural University, Nanjing, P. R. China;
** Corresponding author: zhangxuanhao@njau.edu.cn*

INTRODUCTION

Polylactic acid (PLA) has received global attention due to its good biodegradability. In contrast with other synthetic materials, PLA is biodegradable and can be completely removed by microorganisms in nature after use. Although PLA is recyclable, its high brittleness, long degradation cycle, and high price are obstacles to its application. Because the deterioration of plastics damages the environment, many countries have tried to reduce their dependence on fossil fuel-based polymers, and PLA has received increased attention due to its degradability. Hubbe *et al.* (2021) considered the decomposition properties of PLA and PHB packaging materials. The review showed that the use of biodegradable cellulose reinforced particles could not only enhance the strength, but also make the bioplastics expand, subjecting them to abiotic decomposition. Masirek *et al*. (2007) found that hemp reduced the elongation at break of PLA materials. The 10 wt% hemp/PLA composites (HF/PLA-CM) showed higher torque than pure PLA. Nuthong *et al*. (2013) studied the effects of bamboo fiber, Gyabgon grass fiber, and coconut fiber on the impact properties of PLA composites. The results showed that the impact strength of natural fiber reinforced PLA composites decreased as fiber content increased. The maximum impact strength reduction of bamboo fiber/PLA composites, vetiver fiber/PLA composites, and coconut fiber/PLA composites were 23.8%, 27.3%, and 56.2%, respectively. Porras and Maranon (2012) studied the mechanical properties of PLA laminated composites of

bamboo fabric. The results showed that the breaking force of plain bamboo fabric in the weft direction was greater than that of the warp direction.

In addition, a third material and modification can be used. Huda *et al*. (2008) found that silane-treated fiber (FIBSI) reinforced composites and alkali-treated fiber (FIBNA) reinforced composites had better mechanical properties than untreated fiber (FIB) reinforced composites. Komal *et al*. (2020) studied short banana fiber/PLA biocomposites and showed that fiber pull-out and breakage were the main reasons for biocomposite destruction. Hashima *et al*. (2010) used polyglycidyl methacrylate (EGMA), a reactive compatibilizer, to blend styrene-butadiene-styrene block copolymer (SEBS) to toughen PLA. The results showed that SEBS improved the high temperature resistance and heat aging resistance of the material.

Sodium alginate (SA) is a by-product of extracting iodine and mannitol from kelp or the sargassum of brown algae. In aqueous solutions, SA has high viscosity and has been used as a food thickener, stabilizer, and emulsifier (Lu *et al*. 2014; Jochen *et al*. 2015; Deepa *et al*. 2020). It is of great significance to explore the addition of natural biological glue to prepare biodegradable materials so as to reduce the amount of polylactic acid. To explore the effect of natural biological gum SA on wheat straw/PLA composites, PLA was used as a matrix, plant fiber-wheat straw was added, and SA was used as the third component (biological adhesive).

EXPERIMENTAL

Materials

Polylactic acid (Basic industrial grade, MFI: 12-15 g/ 2.16 kg, 190 °C, 10 min) was produced in Shenzhen Guanghua Weiye Industrial Co., Ltd. (Shenzhen, China). It had a particle size of 100-mesh and was used as a matrix. Wheat straw was purchased from the Chinese market (Nanjing, China) and the crushed grain size was 100-mesh. Sodium alginate was produced by Shanlong Biotechnology Co., Ltd. (Shenzhen, China), and it had a particle size of 200-mesh.

Preparation Method of Wheat Straw/PLA Composites

The PLA and SA content accounted for 50% of the total mass fraction, and SA with different contents (0, 5%, 10%, and 15% by mass) was mixed. Sodium alginate was added to reduce the amount of PLA. Wheat straw powder constituted 50% of the total mass fraction. Table 1 shows the formula of the composites.

Table 1. The Formula of Wheat Straw/PLA Composites with Different SA Contents

Sample Number	SA Content (%)	Wheat Straw Content (%)	PLA Content (%)
1	0	50	50
2	5	50	45
3	10	50	40
4	15	50	35

The components of the composites were mixed in a SBH-5L three-dimensional linkage mixer (Nanjing Xinbao Mechanical and Electrical equipment Industry Co., Ltd., Nanjing, China) at room temperature for 10 min until they were well mixed. Then, they were dried in an oven for 6 h. Next, the four kinds of composites were prepared *via* injection molding, and the injection molding temperature was 180 °C.

Analytical Procedures

Mechanical properties test

The tensile strengths of the four kinds of composites were tested with a CMT6104 universal testing machine (Metz Industrial System (China) Co., Ltd., Shanghai, China) according to GB/T 1040.1 (2018). The stretching speed was 2 mm/min. The impact strengths of the four kinds of composites were tested *via* an XJJ-5 impact tester (Chengde Jinjian Testing Instrument Co., Ltd., Chengde, China) according to GB/T 1843 (2008). All the above experiments were carried out at room temperature, and the average results of three experiments were taken.

Microstructure analysis

The microphase structures of the tensile sections of the four kinds of composites were observed *via* SEM. The tensile fracture surface was treated with a Hitachi E1010 ion sputtering apparatus (Tokyo, Japan) for 1 min, and the tensile sections were observed by field emission SEM (Smur4800, Hitachi, Tokyo, Japan).

Hygroscopicity test

The hygroscopicities of the four kinds of composites were tested with an HPX-160BSH-III constant temperature and humidity box (Dongguan Lixian Instrument Technology Co., Ltd., Dongguan, China) in accordance with GB/T 20312 (2006). The time points of moisture absorption measurement were 6, 18, 42, 66, 114, 138, and 162 h. The temperature was 23 ± 0.5 °C, and the relative humidity was 95%. The composites were taken out and weighed regularly. The moisture absorption extents were calculated with use of Eq. 1,

$$u = \frac{m - m_0}{m_0} \times 100\% \quad (1)$$

where u is the moisture absorption extent (%), m is the mass of the sample after moisture absorption (g), and m_0 is the mass of the dry sample (g).

Thermal stability analysis

In the presence of argon, the thermogravimetric (TG) curves of the composites were measured by a comprehensive thermal analyzer (NETZSCH STA449 F3 Jupiter, Netzsch, Shanghai, China). The thermal stabilities of the four kinds of composites were analyzed for the heating rate of 20 ℃/min and a temperature range from 30 ℃ to 800 ℃.

FTIR analysis

Firstly, KBr disks of four kinds of composites were prepared by the YP-2 pressing mechanism (Shanghai Mountain Scientific instrument Co., Ltd., Shanghai, China). Then the functional groups of the four kinds of composites were tested with a NicoletiS-10 Fourier transform infrared spectrometer (FTIR) (Seymour Fischer Technology Co., Ltd.,

Shanghai, China). The scanning wavenumber ranged from 4000 cm^{-1} to 400 cm^{-1}, with a resolution of 4 cm^{-1} and 16 scans. Finally, the background noise was removed.

Degradation performance test

The samples of the four kinds of composites were dried for 24 h and buried in wet yellow brown soil (taken from the middle and lower reaches of the Yangtze River, 23 ± 2 ℃, 50 ± 5% relative humidity (RH), PH5.5~6.0) at a depth of 10 cm. After 20 d, the samples were collected, and the images were taken out. Then, they were dried and weighed, and the degradation extents were calculated with Eq. 2,

$$d = \frac{m}{m_0} \times 100\% \quad (2)$$

where d is the degradation extent (%), m_0 is the weight before degradation (g), and m is the weight after degradation (g).

RESULTS AND DISCUSSION

Mechanical Property Test for the Four Kinds of Wheat Straw/PLA Composites

Figure 1a shows the tensile strength of wheat straw/PLA composites with different SA contents. Figure 1 demonstrates that the tensile strength of 0%SA was 10.76 MPa. In addition, the tensile strength of 5% SA increased to 12.44 MPa, which was 15.8% higher than that of 0% SA. However, upon increasing to 10% SA, its strength decreased to 11.08 MPa, which was 5.4% less than that of 5% SA. When SA content reached 15%, the tensile strength of the composites further decreased to 10.44 MPa, which was 19% lower than that of 5% SA. Overall, there was an upward trend followed by a downward trend, and the maximum value was reached at 5% SA.

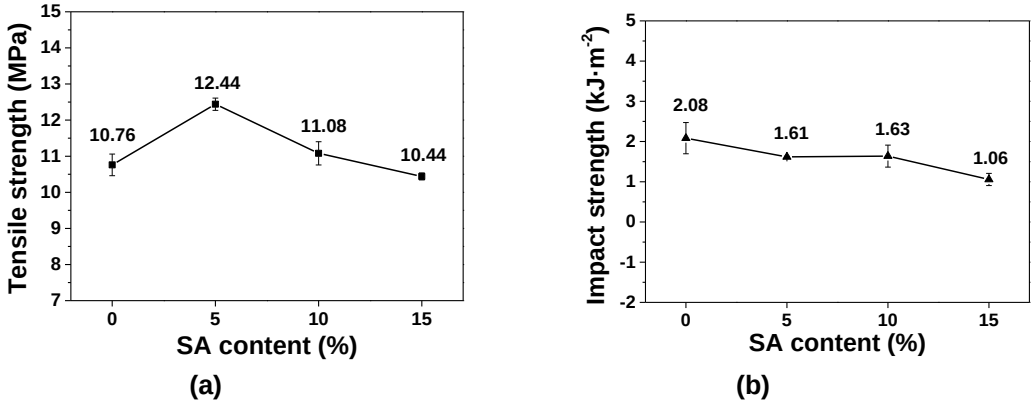

Fig. 1. The tensile strength (a) and impact strength (b) curves of composites with different SA contents

Figure 1b shows the impact strength of wheat straw/PLA composites with different SA contents. In addition, Fig. 1b shows the impact strength of 0%SA as 2.08 $kJ \cdot m^{-2}$. At 5% SA content, the impact strength decreased to 1.61 $kJ \cdot m^{-2}$. At 10% SA content, the

impact strength was largely unchanged. When SA reached 15%, the impact strength of the composites decreased to 1.06 $kJ \cdot m^{-2}$, which constituted a 51.9% decrease relative to 5%SA.

The results showed that the addition of SA greatly influenced the strength and impact toughness of the wheat straw/PLA composites. Overall, the tensile strength and toughness of the composites were better when 5% SA was added. This showed that the addition of a suitable amount (5%) of SA to the composites improved the strength of wheat straw/PLA composites and ensured a certain toughness. This may have been because PLA is a brittle material, while SA acted as a plasticizer, resulting in higher tensile strength than expected during tension. This was because the plasticizer could reduce the brittleness of the composites, so the brittle failure was less of a problem. However, at overly high SA contents, the interfacial bonding properties of the composites were adversely affected because the mechanical properties of natural biological glue were not as good as PLA, and the natural biological glue had higher water absorption and hygroscopicity (Lu *et al*. 2014; Jochen *et al*. 2015). Therefore, the mechanical properties of the composites decreased when SA content was increased beyond optimal level.

Microstructure Analysis for the Four Kinds of Wheat Straw/PLA Composites

Figure 2 shows that there was no obvious void in the 50% wheat straw/PLA composites without SA, but there were several defects, and the fiber was not wrapped tightly enough. The fiber of the composite with 5% SA was almost completely wrapped by the matrix, and there were fewer defects than those without SA. In addition, the surface was smooth. This microstructure enhanced the tensile strength and toughness of the composites. The fiber of the composites with 10% SA was completely wrapped. However, because SA contained a large number of hydroxyl groups, it had strong hydrophilicity. The PLA matrix itself was hydrophobic.

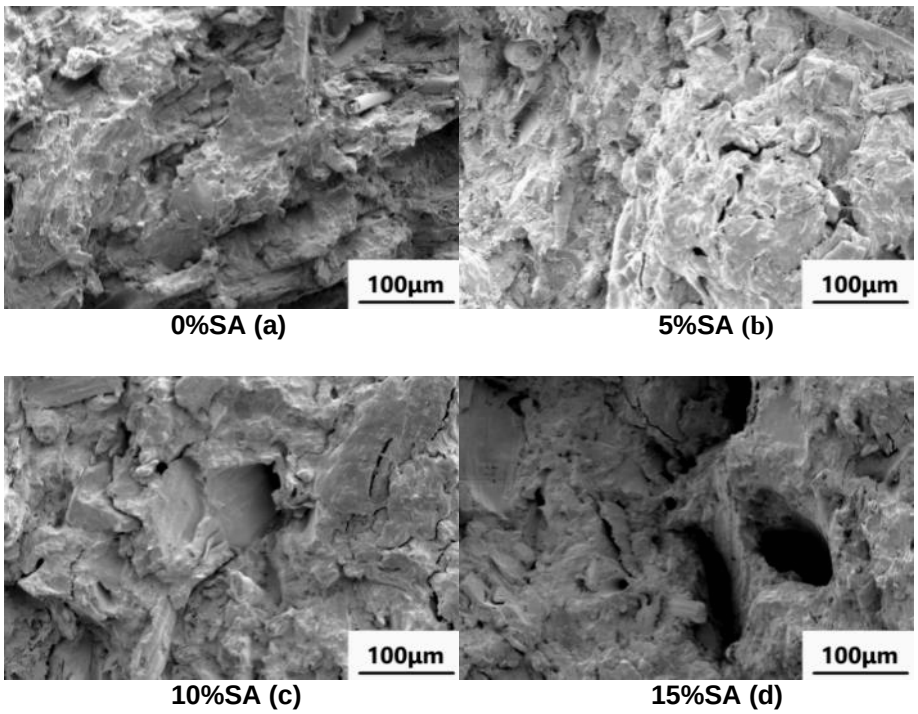

Fig. 2. Microstructure of wheat straw/PLA composites with different SA contents)

After the two phases were mixed, the interfacial adhesion between SA and PLA deteriorated as SA content increased (Liu *et al*. 2019), which resulted in voids and cracks. Similarly, when the SA content in Fig. 2d was 15%, the binding force of the two phases was worse, and the voids and defects were more prominent. This limited the transfer of stress and facilitated stress accumulation, which triggered stress failure and further reduced the tensile strength (Jiang *et al*. 2019).

Due to viscous action, an appropriate amount of SA reduced the interfacial voids and defects in the composites, which resulted in an increase in tensile strength. However, due to the hydrophilicity of SA and the hydrophobicity of PLA, excessive SA led to poor interfacial bonding, increased voids and defects, and increased molecular chain flow resistance, which led to the decreases in composite tensile strength and toughness.

Hygroscopicity Test for the Four Kinds of Wheat Straw/PLA Composites

Figure 3 shows the moisture absorption extent of wheat straw/PLA composites with different SA contents after 7 d of moisture absorption. Figure 3 shows that the moisture absorption of wheat straw/PLA composites with 5% SA content was similar to that of composites without SA, both of which had lower moisture absorption extents than those of 15% SA composites and 10% SA composites.

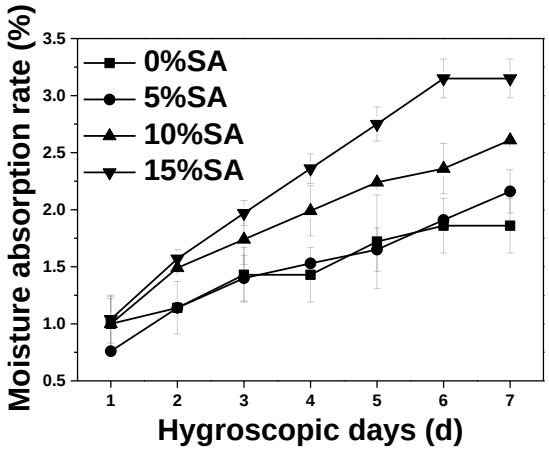

Fig. 3. Moisture absorption extent of wheat straw/PLA composites with different SA contents

In addition, Fig. 3 shows that the moisture absorption extents of wheat straw/PLA composites with 5% SA did not obviously differ from that of wheat straw/PLA composites without SA. The final moisture absorption extents for the 5%SA composites and 10%SA composites were 1.86% and 2.16%, respectively. Due to the addition of SA, the hygroscopicity of the 10% SA and 15% SA composites increased greatly. However, 5% SA had less hygroscopicity, and the final hygroscopicity was only 16% higher than that of the sample without SA, whereas the final hygroscopicity of the 10% SA and 15% SA composites were 40.3% and 69.3% higher than that of the composite without SA, respectively. Generally, the moisture absorption extents of the composites increased as SA content increased. This was due to the fact that SA had strong moisture absorption. Thus, as SA content increased, the moisture absorption extents of the composites increased. In addition, previous studies had shown that PLA is hydrophobic, while SA showed strong hydrophilicity due to the presence of hydroxyl groups. This caused the polymer mixture to be susceptible to breakdown when exposed to water. As a result, the contact area with water was increased, the ability of retaining water was improved, and the moisture absorption

performance was improved. This phenomenon became more obvious when the content of SA increased, thus improving the moisture absorption of the composites.

Thermal Stability Analysis for the Four Kinds of Wheat Straw/PLA Composites

Figure 4a shows the TG curve of SA. The curve in Fig. 4 was in line with the theory of Vijayakumar *et al*. (1985), which states that the thermal decomposition of SA occurs in four steps. The first step takes place between 60 °C and 100 °C. Xi *et al*. (2000) reported that the loss of bound water occurs in this step. The second step occurs from 220 °C to 280 °C. In the second step, the SA cleavage becomes a stable intermediate, the SA skeleton is broken, and the hydroxyl groups are removed in the form of water molecules. The third step takes place between 300 °C and 370 °C. The intermediate products produced in the second step are further decomposed, and the hydroxyl groups are removed. Then, CO_2 is released and carbonization occurs. Finally, the carbides produced in the third step are further oxidized and decomposed to form the final product of Na_2O. Generally, among the four steps of SA thermal decomposition, the degree of thermal decomposition is the highest in the second and third steps from 220 °C to 370 °C.

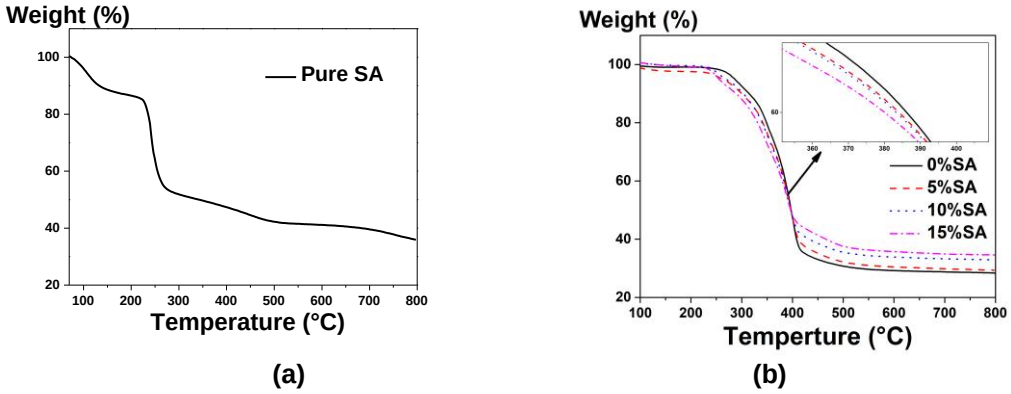

Fig. 4. Material thermal analysis (TG) curves: SA TG curve (a); TG curves of the four kinds of composites (b)

Figure 4b shows the TG curve of the composites with the addition of 0% SA, 5% SA, 10% SA, and 15% SA. The thermal decomposition temperature of the composites was mainly concentrated in the range of 250 to 400 °C, which was consistent with the temperature range of the second and third steps of SA thermal decomposition. In the local magnification diagram of Fig. 4b, the top curve was the TG curve of 0% SA composites, followed by the TG curves of 5% SA, 10% SA, and 15% SA composites. This showed that, as SA content increased, the thermal decomposition extent of the composites increased, the thermal decomposition extent increased, and thermal stability decreased. This was due to the decarboxylation in the second and third steps of SA thermal decomposition. Intermolecular hydrogen bonds were formed between the carbonyl groups in PLA and the hydroxyl groups in SA. In addition, the hydroxyl groups in plant fiber (wheat straw) and PLA could form intermolecular hydrogen bonds (Zhao 2017; Liu *et al*. 2019; Bai *et al*. 2020; Li *et al*. 2021). When the wheat straw fiber combined with PLA to form hydrogen bonds, part of PLA that should have combined with wheat straw formed hydrogen bonds with SA. The hydroxyl groups in SA replaced the hydroxyl groups in wheat straw fiber to form hydrogen bond, which occupied the molecular binding force. Therefore, as SA

content increased, the molecular binding between PLA and wheat straw decreased. When the temperature reached the second stage of SA thermal decomposition, PLA began to decarboxylate, the intermolecular hydrogen bonds disappeared, the interaction between SA and PLA was greatly weakened, and the interface of the composites was maintained only by the force of PLA and wheat straw. As SA content increased, more hydrogen bonds were destroyed by decarboxylation. As PLA decreased, the interaction between PLA and wheat decreased, the bonding force of the interface was reduced, and interfacial compatibility was weakened. Thus, thermal stability declined.

What's more, there was another possible reason. Char would be formed when SA was heated, and the char formation would have a larger scale with the increase of SA content in the composite. This change suggested that when the SA thermally decomposed (starting near to 300°C), the reactive species interacted with other chemical species to form recalcitrant chemical structures. With the increase of SA content, this phenomenon became more obvious, which increased the amount of char remaining at high temperatures.

FTIR Analysis for Four Kinds of Wheat Straw/PLA Composites

Figure 5a shows the infrared spectrum of wheat straw/PLA composites with different SA contents (4000 to 400 cm^{-1}). Figure 5a shows that the absorption peaks of wheat straw/PLA composites with different SA contents were similar, and the main absorption peaks were at 3300 to 3500 cm^{-1}. The broad absorption peak of 3300 to 3500 cm^{-1} was the stretching vibration peak of intramolecular hydroxyl groups (O-H). Plant fiber contained cellulose carboxyl groups (Yu *et al*. 2013). Polylactic acid contained carbonyl groups. The carbonyl groups combined with hydroxyl groups to form intermolecular hydrogen bonds. Figure 5b shows the infrared spectra of wheat straw/PLA composites with different SA contents (4000 to 2500 cm^{-1}).

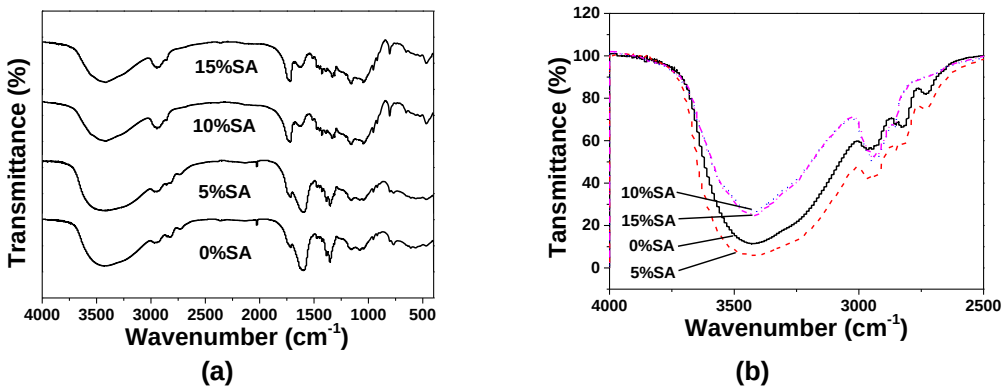

Fig. 5. Infrared spectra of wheat straw/PLA composites with different contents of SA: 4000 to 400 cm^{-1} (a); 4000 to 2500 cm^{-1} (b)

At the bottom of the picture is the infrared spectrum curve of 5% SA composite, followed by the infrared spectrum curve of 0% SA, 15% SA, and 10% SA composites, respectively. This showed that the absorption peak of 5% SA composite was the strongest in the range of 4000 to 2500 cm^{-1}, followed by 0% SA, 15% SA, and 10% SA composites. The enhancement of the absorption peak indicated that hydrogen bonds had formed (Zhang *et al*. 2016; Li 2019; Li *et al*. 2019). Therefore, the addition of 5% SA increased hydrogen bonding and enhanced interfacial compatibility. In contrast, the addition of 10% SA and 15% SA reduces hydrogen bonding, which results in poor interfacial compatibility (Zhang

et al. 2018). This was consistent with the high tensile strength, and low hygroscopicity of the composites with 5% SA. This showed that the wheat straw/PLA composites with 5% SA had excellent properties.

In addition, Fig. 5a shows that there was a characteristic peak of carbonyl groups near the wavenumber segment 1740 cm^{-1} (C=O) , which was the carbonyl vibration peak of PLA. The asymmetric and symmetrical bending vibration absorption peaks of PLA were near the wavenumbers of 1460 and 1382 cm^{-1}. The above absorption peaks were consistent with the theoretical functional groups of the materials.

Degradation Performance Test for Four Kinds of Wheat Straw/PLA Composites

Figure 6 shows the appearance of wheat straw/PLA composites with different SA contents after 20 d of degradation buried in wet soil. Figure 7 shows the degradation percentage of wheat straw/PLA composites with different SA contents.

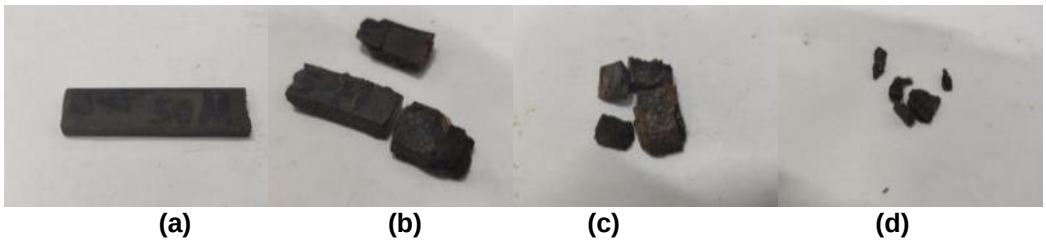

Fig. 6. The appearance of wheat straw/PLA composites with different content of SA after degradation: 0%SA (a); 5%SA (b); 10%SA (c); 15%SA (d)

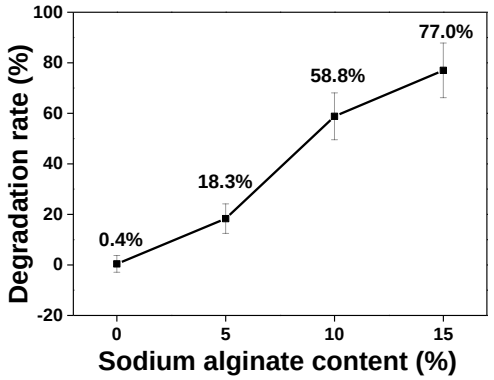

Fig. 7. Chart of degradation percentage of wheat straw/PLA composites with different SA content

Figures 6 and 7 show that the appearance of the composites without SA did not change after 20 d of degradation, and its degradation extent was 0.4%, which indicated that it was not degraded after 20 d. This was in line with Pradhan *et al*. (2010), as they found that the degradation period of wheat straw/PLA composites was 45 d. The composites with SA were degraded to different degrees after 20 d of burial. The 5% SA composites softened, had cracks and 1 to 2 fractures on the surface, and their degradation extent was 18.3%. The surface of the 10% SA composites cracked, which resulted in many fractures and fragments, and the degradation extent was 58.8%. The 15% SA composites were

completely fragmented and difficult to remove from the soil, and the degradation extent was 77%.

These results showed that the addition of SA improved the degradability of wheat straw/PLA composites. As the amount of SA increased, the degradability of wheat straw/PLA composites increased. This was because the decomposition of the PLA matrix was mainly hydrolyzed (Zhang *et al*. 2020), and the addition of SA increased the moisture absorption and water absorption extents of the composites.

CONCLUSIONS

1. The addition of 5% sodium alginate (SA) increased the tensile strength of wheat straw/(poly-(lactic acid)) (PLA) composites, and the tensile strength of 5% SA composites were 15.8%, 5.4%, and 19% higher than the 0% SA, 10% SA, and 15% SA composites, respectively. The impact strength and hygroscopicity of the composites had acceptable change relative to the composites without SA. The impact strength of 5% SA was only 28% lower than that of 0% SA, but the impact strength of 5% SA was 51.9% higher than that of 15% SA.
2. The addition of SA improved the degradability of wheat straw/PLA composites. As SA content increased, degradability increased greatly. The 5% SA composites degraded and broke after being buried in wet soil for 20 d. The 15% SA composites degraded into fragments after 20 d in a wet soil landfill. In addition, the degradation extents of 0% SA, 5% SA, 10% SA, and 15% SA composites were 0.4%, 18.3%, 58.8%, and 77.0%, respectively. Therefore, the addition of SA increased the abiotic decomposition extent of the composites.

ACKNOWLEDGEMENTS

This work was financially supported by the Fundamental Research Funds for the Central Universities (Y0201800586) and Regional Cooperative Innovation in Autonomous Regions (2019E0241).

REFERENCES CITED

Bai, S., Han, C., Ni, Z., Ni, Y., Lyu, Y., and Ye, X. (2020). "Effect of polyethylene glycol (PEG) on properties of the surface modified cellulose nanofiber (CNF)/polylactic acid (PLA) composite," *Journal of Forestry Engineering* 5(2), 62-68. DOI: 10.13360/j.issn.2096-1359.201906031

Deepa, B., Abraham, E., Cordeiro, N., Faria, M., Primc, G., Pottathara, Y., Leskovšek, M., Gorjanc, M., Mozetič, M., and Thomas, S., *et al.* (2020). "Nanofibrils *vs* nanocrystals bio-nanocomposites based on sodium alginate matrix: An improved-performance study," *Heliyon* 6(2), e03266. DOI: 10.1016/j.heliyon.2020.e03266

GB/T 1040.1 (2018). "Plastics – Determination of tensile properties – Part 1: General principles," Standardization Administration of China, Beijing, China.

GB/T 1843 (2008). "Plastics – Determination of izod impact strength," Standardization Administration of China, Beijing, China.

GB/T 20312 (2006). "Hygrothermal performance of building materials and products-Determination of hygroscopic sorption properties," Standardization Administration of China, Beijing, China.

Hashima, K., Nishitsuji, S., and Inoue, T. (2010). "Structure-properties of super-tough PLA alloy with excellent heat resistance," *Polymer* 51(17), 3934-3939. DOI: 10.1016/j.polymer.2010.06.045

Hubbe, M. A., Lavoine, N., Lucia, L. A., and Dou, C. (2021). "Formulating bioplastic composites for biodegradability, recycling, and performance: A review," *BioResources* 16(1), 2021-2083.

Huda, M. S., Drzal, L. T., Mohanty, A. K., and Misra, M. (2008). "Effect of fiber surface-treatments on the properties of laminated biocomposites from poly(lactic acid) (PLA) and kenaf fibers," *Composites Science and Technology* 68(2), 424-432. DOI: 10.1016/j.compscitech.2007.06.022

Jiang, L., He, C., Wang, L., and Jiang, C. (2019). "Comparison of seawater corrosion resistance of four types of plant fibers/high-density polyethylene composites," *Acta Materiae Compositae Sinica* 36(7), 1625-1632. DOI: 10.13801/j.cnki.fhclxb.20181023.001

Jochen, S., Volker, S., and Bernd, R. (2015). "Bacterial exopolysaccharides: Biosynthesis pathways and engineering strategies," *Frontiers in Microbiology* 6, article no. 496. DOI: 10.3389/fmicb.2015.00496

Komal, U. K., Lila, M. K., and Singh, I. (2020). "PLA/banana fiber based sustainable biocomposites: A manufacturing perspective," *Composites Part B: Engineering* 180, Article ID 107535. DOI: 10.1016/j.compositesb.2019.107535

Li, N., Chen, H., Yang, S., Cao, C., Shao, L., and Liu, Y. (2019). "Study on TCF short sequence bleaching of poplar kraft pulp," *Paper Science and Technology* 38(6), 8-13. DOI: 10.19696/j.issn1671-4571.2019.6.002

Li, Y., Zhou, S., Lu, C., Luo, Y., and Bai, X. (2021). "Effect of PP-g-MAH on properties and morphologies of nylon 6/carbon black composites," *Engineering Plastics Application* 49(1), 44-48. DOI: 10.3969/j.issn.1001-3539.2021.01.009

Li, Z. (2019). *Study on Poisoning and Anti-poisoning Mechanism of CH_4-SCR on In/H-Beta Catalyst*, Ph.D. Thesis, Harbin Institute of Technology, Harbin, China. DOI: 10.27061/d.cnki.ghgdu.2019.002317

Liu, Z., Nie, S., Gong, M., Qin, T., Zhu, Y., Wan, L., and Zhang, Y. (2019). "Preparation and properties of lignin/wood flour/PLA composite," *Plastics* 48(2), 8-13.

Lu, D., Xu, Q., and Wang, W. (2014). "Research advancement of gel mechanism of alginate and its application in food," *Food and Nutrition in China* 20(10), 43-46. DOI: 10.3969/j.issn.1006-9577.2014.10.011

Masirek, R., Piorkowska, E., Galeski, A., and Mucha, M. (2007). "Influence of thermal history on the nonisothermal crystallization of poly(L-lactide)," *Journal of Applied Polymer Science* 105(1), 282-290. DOI: 10.1002/app.26047

Nuthong, W., Uawongsuwan, P., Pivsa-Art, W., and Hamada, H. (2013). "Impact property of flexible epoxy treated natural fiber reinforced PLA composites," *Energy Procedia* 34, 839-847. DOI: 10.1016/j.egypro.2013.06.820

Porras, A., and Maranon, A. (2012). "Development and characterization of a laminate composite material from polylactic acid (PLA) and woven bamboo fabric,"

Composites Part B: Engineering 43(7), 2782-2788. DOI: 10.1016/j.compositesb.2012.04.039

Pradhan, R., Misra, M., Erickson, L., and Mohanty, A. (2010). "Compostability and biodegradation study of PLA–wheat straw and PLA–soy straw based green composites in simulated composting bioreactor," *Bioresource Technology* 101(21), 8489-8491. DOI: 10.1016/j.biortech.2010.06.053

Vijayakumar, M. T., Reddy, C. R., and Joseph, K. T. (1985). "Grafting of poly(glycidyl methacrylate) onto alginic acid," *European Polymer Journal* 21(4), 415-419. DOI: 10.1016/0014-3057(85)90201-0

Xi, G., Tian, S., Cheng, Q., and Zhang, Q. (2000). "Studies on thermal dissociation of sodium alginate," *Chemical World* (5), 254-258. DOI: 10.19500/j.cnki.0367-6358.2000.05.009

Yu, M., He, C., Zhang, H., Hou, R., and Xue, J. (2013). "Effect of different pretreatments on tribological properties of wheat straw/polypropylene composites," *Transactions of the Chinese Society for Agricultural Machinery* 44(7), 138-143. DOI: 10.6041/j.issn.1000-1298.2013.07.024

Zhang, C., Ying, Q., Wu, J., Kang, L., Liu, F., Ba, N., and Yan, Y. (2020). "Study of the characterizations of polyhydroxylbutyrate valerate (PHBV) and polylactic acid (PLA)," *Journal of Green Science and Technology* 2020(20), 152-154, 170. DOI: 10.16663/j.cnki.lskj.2020.20.049

Zhang, J., He, C., Tang, H., Fu, J., and Wang, M. (2016). "Performance comparison of three kinds of plant fibers modified polylactic acid composites," *Engineering Plastics Application* 44(11), 12-17. DOI: 10.3969/j.issn.1001-3539.2016.11.003

Zhang, N., Zhang, J., He, W., and Wang, L. (2018). "Applicability of modified collagen to pigments fixing for Chinese calligraphy and paintings," *Sciences of Conservation and Archaeology* 30(3), 14-20. DOI: 10.16334/j.cnki.cn31-1652/k.2018.03.003

Zhao, Y. (2017). *Study on Preparation and Properties of Oil-impregnated Monomer Casting Nylon/graphene Oxide Composites*, Hebei University of Technology, Tianjin, China.

Article submitted: March 4, 2021; Peer review completed: April 17, 2021; Revised version received and accepted: June 15, 2021; Published: July 13, 2021.

DOI: 10.15376/biores.16.3.6003-6014